CARBON 63 (2013) 397–403

Available at www.sciencedirect.com

SciVerse ScienceDirect

journal homepage: www.elsevier.com/locate/carbon

# A stable silicon/graphene composite using solvent exchange method as anode material for lithium ion batteries

*Deniz P. Wong* [a,c,d], *Han-Ping Tseng* [e], *Yit-Tsong Chen* [b,c], *Bing-Joe Hwang* [e], *Li-Chyong Chen* [a,*], *Kuei-Hsien Chen* [a,b,*]

[a] *Center for Condensed Matter Sciences, National Taiwan University, No. 1 Sec. 4, Roosevelt Rd., Taipei 10617, Taiwan*
[b] *Institute of Atomic and Molecular Sciences, Academia Sinica, No. 1 Sec. 4, Roosevelt Rd., Taipei 10617, Taiwan*
[c] *Department of Chemistry, National Taiwan University, No. 1 Sec. 4, Roosevelt Rd., Taipei 10617, Taiwan*
[d] *Nanoscience and Technology Program, Taiwan International Graduate Program, Academia Sinica, Taipei 11529, Taiwan*
[e] *Department of Chemical Engineering, National Taiwan University of Science and Technology, 43 Keelung Road, Section 4, Taipei 10617, Taiwan*

ARTICLE INFO

*Article history:*
Received 10 May 2013
Accepted 30 June 2013
Available online 4 July 2013

ABSTRACT

Current research has demonstrated the combination of the high theoretical capacity offered by silicon nanoparticles (Si NPs) with graphene-based matrices in order to produce a high energy density and stable lithium ion battery system. However, Si NPs do not mix well with graphene oxide aqueous suspensions and thus create severe segregation of the materials. In this letter, we propose a simple, cost-effective and commercially-viable solvent exchange process to improve the interaction of the Si NPs in poor solvent environments such as in aqueous media. Using N-methylpyrrolidone (NMP) to disperse the Si NPs and followed by a solvent exchange process, we are able to improve the dispersion and stability of Si NPs in aqueous graphene oxide aqueous suspension. Consequently, this also improves the output and the stability of the lithium ion battery using the aforementioned composite system.



## 1. Introduction

In the past few decades, lithium ion batteries (LiBs) have increased in popularity and usage since it could provide high energy density storage [1,2], but there is still a strong desire to improve many aspects of LiBs, including cost, safety, energy density, capacity, cycle life, and rate capability. Furthermore, the recent interest in using LiBs for automobiles has also intensified the search for new class of materials that can achieve higher energy density while maintaining a longer cycle life [3,4].

Silicon has been known to accommodate the most number of lithium when lithiated among known elements or compounds studied in the field of rechargeable batteries. As such, silicon is an attractive candidate anode material for lithium ion batteries with its theoretical capacity of 4200 mAh/g [5,6]. However, the major drawbacks of using silicon are the large volume change that occurs during the lithiating and delithiating process [7] and its low intrinsic electrical

* *Corresponding author at:* Center for Condensed Matter Sciences, National Taiwan University, No. 1 Sec. 4, Roosevelt Rd., Taipei 10617, Taiwan (L.-C. Chen), Institute of Atomic and Molecular Sciences, Academia Sinica, No. 1 Sec. 4, Roosevelt Rd., Taipei 10617, Taiwan (K.-H. Chen). Fax: +886 2 33665280.
E-mail addresses: chenlc@ntu.edu.tw (L.-C. Chen), chenkh@pub.iams.sinica.edu.tw (K.-H. Chen).
0008-6223/$ - see front matter 
http://dx.doi.org/10.1016/j.carbon.2013.06.095

conductivity [8,9]. In order to mitigate this problem, several studies have proved the utility of nanoparticles [10], nanowires [11], nanotubes [12] and other nanostructured -based materials [13]. Furthermore, carbon-based Si composites are also being developed in order to improve the conductivity of the active material [14].

Recently, Si–graphene composites offer an attractive approach in decreasing the problems brought about by using solely pure elemental silicon [15–17]. Due to the nature of graphene, the two-dimensional material offers a conducting channel for electrons from the silicon and at the same time can also act as a buffering matrix to the accompanying volume expansion that arises during the lithiation of the silicon nanoparticles (Si NPs). Various approaches that one can follow to achieve composites with improved lithium ion battery performance have been made. One of the easiest approaches is to mix nanostructured silicon in graphene oxide (GO) aqueous suspension to formulate the composite mixture for the battery application. However, when preparing a suspension of the composites, the dispersion and stability of Si NPs in the aqueous media usually presents a problem [18]. This causes the formation of non-uniform Si NPs graphene composites leading to a limited electrochemical performance. Therefore, a new process is necessary to improve the mixing properties of the materials.

The attractiveness of the composite approach is the low cost and ease in integrating such process into the current coating methods applied in the lithium ion battery industry [19]. Thus, the new process should take the advantages of the current approach while trying to solve the dispersion problems of the Si NPs in a specific media. Various approaches involving the use of chemical functionalization on the graphene to capture Si NPs [20] and the use of cationic polymer as a mediator for self-assembled electrostatic attraction [21] between Si NPs and graphene have shown improvements in the uniformity of the dispersion while offering an improved battery performance. However, by understanding the interaction of Si NPs in various solvents, we have come up with a proposed method that does not require additional chemical functionalization step [20,22] or polymer additive [21] to achieve a homogeneous Si NPs–graphene composite.

In this study, we proposed the use of a solvent exchange method [23] that enables the Si NPs to readily disperse and stabilize in the GO aqueous suspension. This involves the use of an appropriate solvent, N-methyl-2-pyrolidone (NMP) and other polar aprotic solvents including acetonitrile (ACN) and acetone (ACE) that can disperse and stabilize the Si NPs in suspension. Improved homogeneity of the Si NPs-GO suspension, which translates to uniform Si NPs–GO composite, can be achieved. In this way, no additional materials or chemical modifications are needed. The stable suspension is then used to form a composite blend for lithium-ion battery application. Although the use of NMP, an organic solvent, adds to the cost of the initial process, it should be noted that NMP can easily be recovered and reused after the solvent exchange method. After separating the SiNPs for the composite suspension, succeeding solvent exchange process can still be done using the remaining supernatant.

## 2. Experimental section

### 2.1. *Preparation of GO suspension [24]*

GO was prepared using a modified Hummers and Offeman's method [25]. In a typical reaction, graphite (2.5 g, ITRI), sodium nitrate ($NaNO_3$, 2.5 g, reagent grade, Aldrich) and sulfuric acid ($H_2SO_4$, 115 mL, Acros) were stirred together in an ice bath. Potassium permanganate ($KMnO_4$, 7.5 g, Aldrich) was slowly added while stirring, and the rate of addition was controlled to prevent the temperature of the mixture from exceeding 20 °C.

The mixture was then transferred to a 35 °C water bath and stirred for about 0.5 h, forming a thick paste. Subsequently, de-ionized water (115 mL) was added gradually, causing an increase in temperature to 98 °C. After 15 min, the mixture was further treated with de-ionized water (350 mL) and $H_2O_2$ solution (30%, 25 mL). The warm solution was then filtered and washed with de-ionized water until the pH was 7 and dried at 65 °C under vacuum.

### 2.2. *Solvent exchange process*

Silicon nanoparticles (40 mg, Aldrich, <100 nm), were first dispersed in 1-methyl-2-pyrrolidinone (NMP) (Acros) and agitated subsequently using an ultrasonic bath for 1 h. The silicon nanoparticles were recovered after undergoing high speed centrifugation (24,000 RPM) for 15 min. This is followed by the addition of 2.3 g of 0.5% (w/v) GO aqueous suspension to Si NPs obtained after centrifugation to make up a ratio of 3.5:1 by weight of Si NPs to GO. The suspension was then agitated under ultrasonic bath for another hour prior to usage.

### 2.3. *Preparation of active material slurry and electrode fabrication*

The Si NPs–GO composite was obtained after removing the water in a rotary evaporator. The composite was further treated by converting the GO to reduced graphene oxide (rGO) through a thermal reduction process at 500 °C under $H_2$/Ar (5:95 v/v) atmosphere. After the formation of the Si NPs–rGO composite, the products were immersed in 10% hydrofluoric acid solution to remove the oxides on the surface of the silicon. After filtration, the composites were dried in vacuum overnight. The final ratio of SiNPs to rGO is 1:1 by weight determined by thermogravimetric analysis (TGA) (see Fig. S1 in the Supporting information). The composites were mixed with Super P (Timcal) and sodium carboxymethylcellulose (Aldrich) in a ratio of 80:10:10. The formulated slurry mixture was then coated on copper foil (99.9%, ITRI) and prepared for CR2032 coin cell type of fabrication. The electrolyte was 1 M $LiPF_6$ in EC/DMC (1:1 v/v) (Tomiyama). Polyethylene films (Asahi N910) were utilized as separators and pure lithium metal foil was used as the counter electrode. The electrodes were assembled in an argon-filled glove box.

### 2.4. *Dispersion and electrochemical characterization*

The particle size of the Si NPs in various solvents was measured using Malvern Zetasizer Nano S while the absorption

spectra were taken using Jasco V-630 UV–Vis spectrometer. The Fourier transform infrared spectra (FTIR) were taken using Thermo Nicolet 6700-FTIR in attenuated total reflectance (ATR) mode. The discharge and charge measurements of the batteries were performed on an Arbin BT2000 system in the fixed voltage window between 0.05 and 1.2 V at room temperature. The AC impedance was measured at an Autolab electrochemical workstation (PGSTAT302 N), with frequency range and voltage amplitude set as 1 MHz to 0.01 Hz and 10 mV, respectively. Raman spectra were obtained using Horiba Jobin–Yvon Horiba 800UV confocal Raman spectrometer at excitation source of 633 nm. X-ray diffraction (XRD) measurements were conducted on a Bruker, D2 Phaser. The thermal gravimetric analysis was done using Perkin Elmer TGA 4000 while scanning electron microscopy (SEM) images were obtained using JEOL 6700 FE-SEM).

## 3. Results and discussion

### 3.1. *Characterization and evaluation of the solvent exchange process*

To demonstrate the effectiveness of the treatment, solvent exchange process was applied to Si NPs on three different kinds of solvent (2-propanol, water and toluene). Our target solvent in this case is water while 2-propanol will act as our positive control and toluene as our negative control [26]. We hypothesized that the solvent exchange process only works to improve the dispersion of Si NPs in polar solvents. Hence, aside from water, dispersion of Si NPs in 2-propanol (a polar solvent) will also improve while that in toluene (a non-polar solvent) will not work.

From Fig. 1a, it can be first observed that untreated Si NPs, without undergoing the solvent exchange process, show poor dispersion and/or stability to all of the three solvents after letting the suspension stand for one day. On the other hand, after undergoing the solvent exchange process, the Si NPs clearly have better dispersion and stability in 2-propanol and water while maintaining a poor dispersion in toluene. This observation indicated that the polar characteristic of the initial solvent used plays a role in improving the dispersion of the Si NPs in succeeding polar solvent.

In NMP, Si NPs have a smaller hydrodynamic diameter from the dynamic light scattering (DLS) measurement (Fig. 1b) compared with the particles dispersed in water even after the solvent exchange process. This shows that Si NPs has better dispersion and stability in NMP. Although signs of aggregates can still be observed after the solvent exchange process, a narrower distribution can be seen compared to the suspension without undergoing the said process. For the untreated sample, it was observed after measurements that large aggregates of Si NP settled on the bottom of the cell. This may explain why no large size was detected during the DLS measurement for the untreated sample.

Fig. 1c shows a quantitative interpretation of the results from the optical photograph (Fig. 1a). Since all three solvents used do not absorb in the visible range, the absorption observed can be attributed solely to the Si NPs. We can take

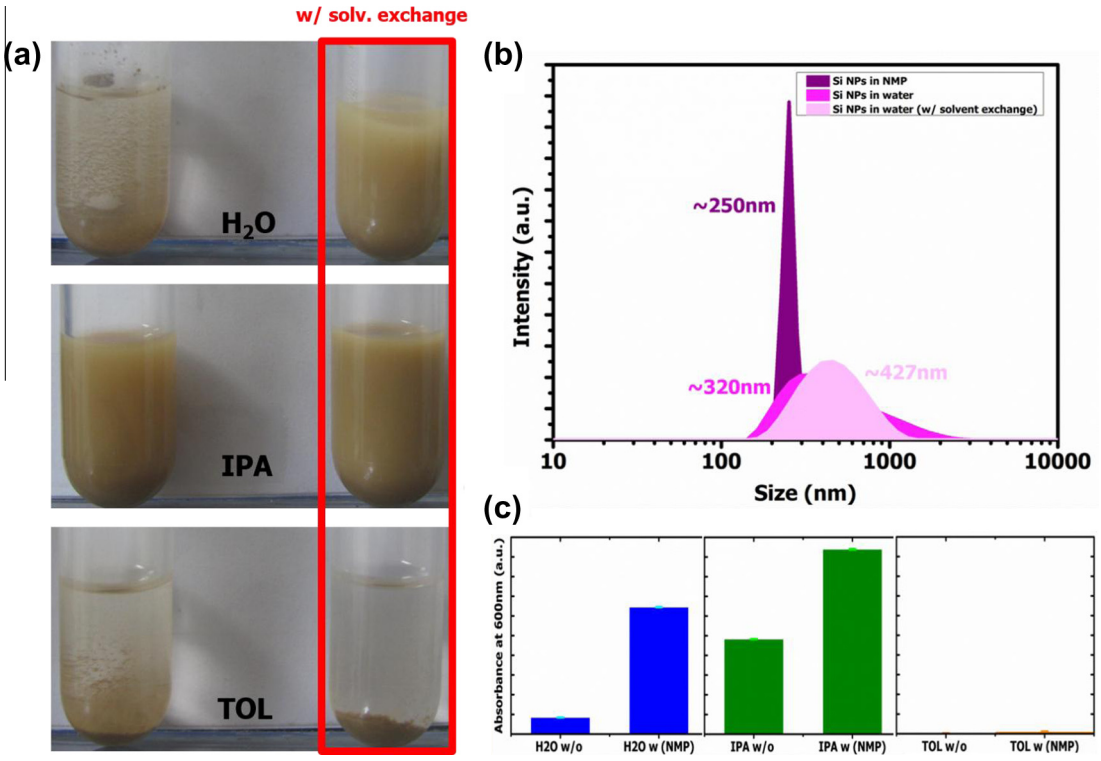


**Fig. 1 – (a) Photographic images of Si NPs dispersed in various solvents (water ($H_2O$), 2-propanol (IPA) and toluene (TOL)) with and without applying the solvent exchange process, (b) dynamic light scattering measurement of Si NPs dispersed in NMP (250 nm), in $H_2O$ with (427 nm) and without (320 nm) the mediation of the solvent exchange process (with indication of the peak center) and (c) absorbance at 600 nm of the diluted supernatant in (a).**

the absorption spectrum of the supernatant (Fig. S2 in SI) to make a semi-quantitative assessment on the effectiveness of the process. Taking the absorbance at 600 nm (arbitrary point), it can be inferred that the process is most effective for 2-propanol followed by water and clearly shows no absorbance from the sample using toluene as solvent. It is clear from the results that the process does not apply to non-polar solvents. This implies that the solvent exchange process makes the surface of the Si NPs polar which explains the improved interaction with polar solvents while maintaining a poor interaction in non-polar solvent. Furthermore, it can also be noted that the dielectric constant of NMP (32.55) is much closer to 2-propanol (20.18) compared to water (80.10) [27]. As such, NMP's polar character is much closer to 2-propanol than water, thus making NMP and 2-propanol more compatible to each other [28].

From the results above, a schematic mechanism can be inferred (Fig. 2). Without undergoing the solvent exchange process (Fig. 2a), Si NPs easily form aggregates. Even under ultrasonic agitation, aggregations are still observed. The aggregation continues to increase as soon as the suspension returns to equilibrium. On the other hand, the solvent exchange method (Fig. 2b) takes advantage of the residual molecules (NMP) that is retained on the surface of the Si NPs due to strong non-bonding interaction (Fig. 2b) between the solvent and the solute. Since NMP molecules are compatible in aqueous media, it improves the dispersion and stability of the particles in water or any other polar solvent previously having poor interaction with Si NPs. Fig. 2c shows the Fourier transform infrared (FTIR) spectrum of the Si NPs after the solvent exchange process (in blue line), which indicates a very weak but clear peak attributed to the carbonyl peak of 1-methyl-2-pyrrolidinone (in black line).

We have also demonstrated the effectiveness of the solvent exchange process using other polar aprotic solvent such as acetonitrile and acetone (Fig. 3). Using these polar aprotic solvents, a big improvement in the dispersion of Si NPs in water can also be observed. Fig. 3b also shows the absorbance of Si NPs at 600 nm in water after undergoing the solvent exchange process.

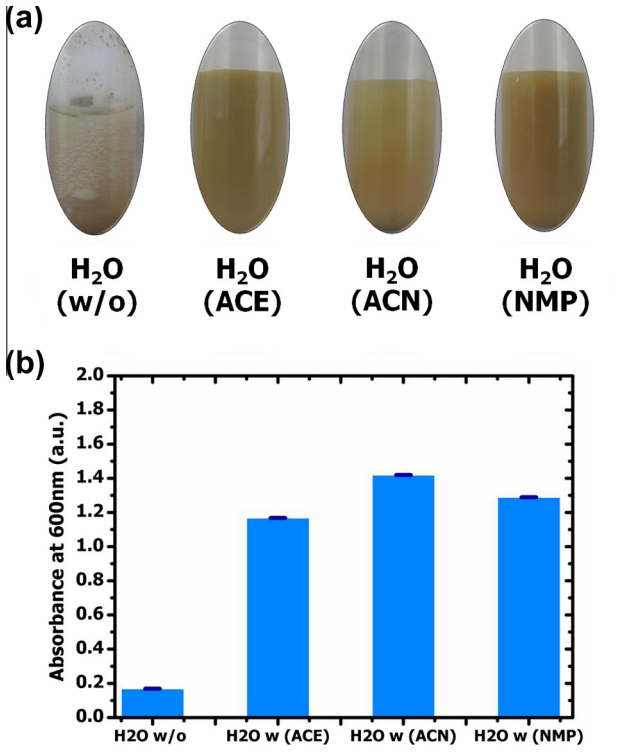


**Fig. 3 – (a) Visible absorption spectra of Si NPs in various solvent after one day. The solutions were diluted 4×. (b) The absorbance of Si NPs at 600 nm in water after undergoing the solvent exchange process.**

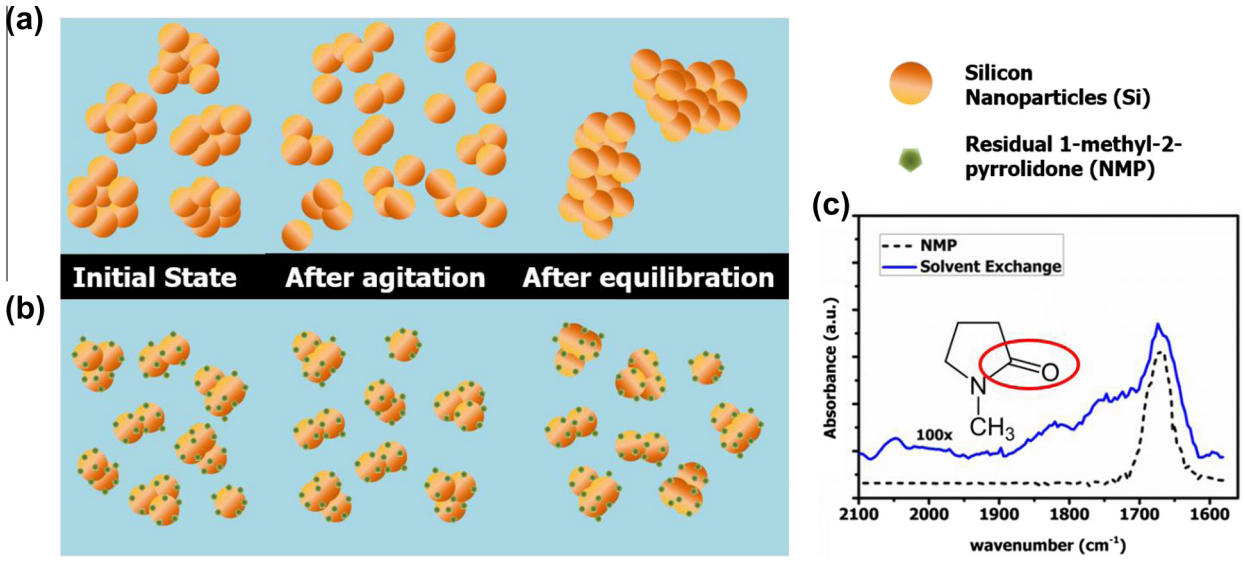


**Fig. 2 – Schematic picture of Si NPs when dispersed in an incompatible solvent (water) (a) before and (b) after undergoing the solvent exchange method. (c) FTIR spectrum of the NMP (dotted line) and Si NPs after the solvent exchange method (solid line).**

### 3.2. *Preparation and characterization of SiNPs – graphene composite*

After improving the dispersion of Si NPs in aqueous media, the same process was applied prior to the addition of Si NPs in the GO aqueous suspension. Fig. 4a shows a more homogeneous composite suspension after applying the treatment. Si NPs are less likely seen floating on the suspension or sticking on the sides of the tube walls. After further agitation, both treated and untreated suspensions were further processed by subjecting the evaporated and dried Si NPs–GO composite to thermal reduction. This converted the carbon component into reduced GO (rGO) and improved its electrical conductivity [29]. XRD pattern (see Fig. S3 in SI) and Raman spectra (see Fig. S4 in SI) have shown no difference on the Si NPs and rGO properties with or without using the solvent exchange process. No apparent morphological difference can also be inferred from the SEM images between two processes after GO reduction (see Fig. S5 in SI). Thus, the process itself doesn't affect the intrinsic properties of both materials. Consequently, the Si NPs–rGO composite was used as a slurry mixture for lithium ion battery testing.

### 3.3. *Lithium-ion battery testing*

The cycling performance (Fig. 4b) shows that without the use of any carbon based material, the capacity fading problem is very serious with almost no capacity after the 30th cycle. Between the composite samples, solvent exchange mediated process clearly shows better stability compared to the untreated sample. Our results have shown an initial capacity of 1264 mAh/g and retention of about 70% after 30 cycles. This is comparable to the results reported in literature which used surface modification [21] or even chemical functionalization [20] on the composite to improve the Si–GO interaction.

Comparing the initial coulombic efficiency of our cells (Fig. 4c), no difference in terms of the effectiveness of lithiation and delithiation is observed. This means that the initial activity of the Si NPs was not compromised even after undergoing various treatments. However, it is clearly seen that as the charge–discharge cycle progresses, pure Si NPs shows an erratic coulombic efficiency which is consistent with the decline in its cyclic performance. On the other hand, no significant differences in the coulombic efficiency were observed on the composite samples. Thus, the difference in terms of the specific capacity of the composite can only be attributed towards the variation of the composite homogeneity prior to the electrical measurement. By normalizing the cycling performance with the amount of Si NPs (see Fig. S6 in SI), a bigger difference can be further observed, showcasing the improvement caused by the solvent exchange process.

In addition, the formation of a homogeneous Si–rGO composite leads to a better performance of the GO as a buffering matrix of the Si NPs while it expands during lithiation. Since the silicon is better spaced between the GO matrices, there is also an improvement in the overall conductivity of the composite system. Our AC impedance measurements further supports the improvement in the composite system after undergoing the solvent exchange process (Fig. 4d). Typically, the semicircle in the mid-frequency range is assigned to the charge transfer resistance [30], therefore it is obvious that the modified composites provides faster charge transfer than

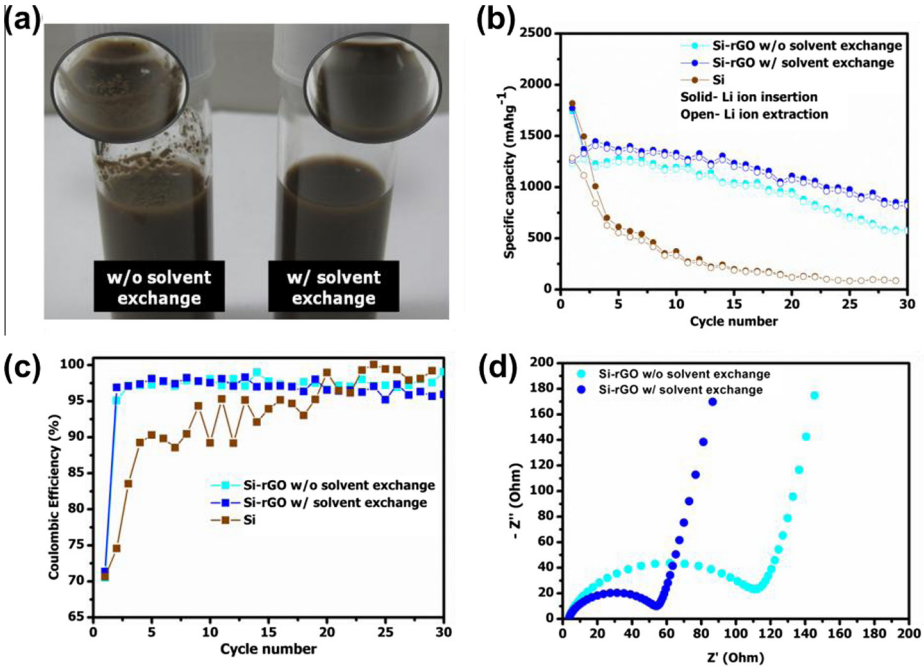


**Fig. 4 – (a) Photographic image of Si–GO composite aqueous suspension with and without Si NPs undergoing solvent exchange process, (b) cycling performance of Si–rGO with and without the use of the solvent exchange process and pure Si NPs at current density of 200 mA/g, (c) comparison of their coulombic efficiencies and (d) Nyquist plots of the two Si–rGO samples.**

the unmodified one due to better dispersion and homogeneity of the Si NPs in the carbon matrix.

## 4. Conclusions

In conclusion, we have demonstrated the improvement in the dispersion and stability of silicon nanoparticles in aqueous suspension using a simple solvent exchange process. Furthermore, we have applied the process to create a stable Si NPs–GO suspension which was later used as an active material in lithium-ion battery application. With the aid of the solvent exchange process, the Si NPs–rGO composite shows an enhanced and more stable performance than the same composite without the aforementioned treatment. The improved capacity is attributed to better dispersion of the silicon nanoparticles within the graphene matrix, which in turn maximizes the function of the carbon material as a conductive additive and elastic matrix. In addition, the obtained capacity of the treated sample shows only a capacity loss of 32% compared to 46% of the untreated sample after 30 cycles. Moreover, the process can also be generally applied to different composite systems that are facing similar compatibility problems. Aggregation of the various components in the composite systems tends to decrease the expected performance of the desired application. However, having specific solutions only to specific systems adds more cost and time to develop. Therefore, finding a general approach to the problem is an ideal solution for this situation.

## Acknowledgments

This work was supported by the Taiwan International Graduate Program and grants from the Institute of Atomic Molecular Sciences, Academia Sinica, Center for Emerging Material and Advanced Devices, National Taiwan University and the National Science Council of Taiwan.

## Appendix A. Supplementary data

Supplementary data associated with this article can be found, in the online version, at http://dx.doi.org/10.1016/j.carbon.2013.06.095.

## REFERENCES

[1] Goodenough JB, Park K-S. The Li-ion rechargeable battery: a perspective. J Am Chem Soc 2013;135(4):1167–76.
[2] Armand M, Tarascon JM. Building better batteries. Nature 2008;451(7179):652–7.
[3] Manthiram A. Materials challenges and opportunities of lithium ion batteries. J Phys Chem Lett 2011;2(3):176–84.
[4] Tarascon JM, Armand M. Issues and challenges facing rechargeable lithium batteries. Nature 2001;414(6861):359–67.
[5] Kasavajjula U, Wang C, Appleby AJ. Nano- and bulk-silicon-based insertion anodes for lithium-ion secondary cells. J Power Sources 2007;163(2):1003–39.
[6] Li H, Huang X, Chen L, Wu Z, Liang Y. A high capacity nano Si composite anode material for lithium rechargeable batteries. Electrochem Solid-State Lett 1999;2(11):547–9.
[7] Jung SC, Choi JW, Han Y-K. Anisotropic volume expansion of crystalline silicon during electrochemical lithium insertion: an atomic level rationale. Nano Lett 2012;12(10):5342–7.
[8] Gu M, Li Y, Li X, Hu S, Zhang X, Xu W, et al. In situ TEM study of lithiation behavior of silicon nanoparticles attached to and embedded in a carbon matrix. ACS Nano 2012;6(9):8439–47.
[9] Chen X, Li X, Ding F, Xu W, Xiao J, Cao Y, et al. Conductive rigid skeleton supported silicon as high-performance Li-ion battery anodes. Nano Lett 2012;12(8):4124–30.
[10] Liu XH, Zhong L, Huang S, Mao SX, Zhu T, Huang JY. Size-dependent fracture of silicon nanoparticles during lithiation. ACS Nano 2012;6(2):1522–31.
[11] Chan CK, Peng H, Liu G, McIlwrath K, Zhang XF, Huggins RA, et al. High-performance lithium battery anodes using silicon nanowires. Nat Nanotechnol 2008;3(1):31–5.
[12] Park M-H, Kim MG, Joo J, Kim K, Kim J, Ahn S, et al. Silicon nanotube battery anodes. Nano Lett 2009;9(11):3844–7.
[13] Chen D, Mei X, Ji G, Lu M, Xie J, Lu J, et al. Reversible lithium-ion storage in silver-treated nanoscale hollow porous silicon particles. Angew Chem Int Ed 2012;51(10):2409–13.
[14] Magasinski A, Dixon P, Hertzberg B, Kvit A, Ayala J, Yushin G. High-performance lithium-ion anodes using a hierarchical bottom-up approach. Nat Mater 2010;9(4):353–8.
[15] Xin S, Guo Y-G, Wan L-J. Nanocarbon networks for advanced rechargeable lithium batteries. Acc Chem Res 2012;45(10):1759–69.
[16] Lee JK, Smith KB, Hayner CM, Kung HH. Silicon nanoparticles-graphene paper composites for Li ion battery anodes. Chem Commun 2010;46(12):2025–7.
[17] Xiang H, Zhang K, Ji G, Lee JY, Zou C, Chen X, et al. Graphene/nanosized silicon composites for lithium battery anodes with improved cycling stability. Carbon 2011;49(5):1787–96.
[18] Bleier A. The roles of van der Waals forces in determining the wetting and dispersion properties of silicon powder. J Phys Chem 1983;87(18):3493–500.
[19] Luo J, Zhao X, Wu J, Jang HD, Kung HH, Huang J. Crumpled graphene-encapsulated Si nanoparticles for lithium ion battery anodes. J Phys Chem Lett 2012;3(13):1824–9.
[20] Yang S, Li G, Zhu Q, Pan Q. Covalent binding of Si nanoparticles to graphene sheets and its influence on lithium storage properties of Si negative electrode. J Mater Chem 2012;22(8):3420–5.
[21] Zhou X, Yin Y-X, Wan L-J, Guo Y-G. Self-assembled nanocomposite of silicon nanoparticles encapsulated in graphene through electrostatic attraction for lithium-ion batteries. Adv Energy Mater 2012;2(9):1086–90.
[22] Zhu Y, Liu W, Zhang X, He J, Chen J, Wang Y, et al. Directing silicon–graphene self-assembly as a core/shell anode for high-performance lithium-ion batteries. Langmuir 2012;29(2):744–9.
[23] Zhang X, Coleman AC, Katsonis N, Browne WR, van Wees BJ, Feringa BL. Dispersion of graphene in ethanol using a simple solvent exchange method. Chem Commun 2010;46(40):7539–41.
[24] Hsu H-C, Shown I, Wei H-Y, Chang Y-C, Du H-Y, Lin Y-G, et al. Graphene oxide as a promising photocatalyst for $CO_2$ to methanol conversion. Nanoscale 2013;5(1):262–8.
[25] Hummers WS, Offeman RE. Preparation of graphitic oxide. J Am Chem Soc 1958;80(6):1339.
[26] Reindl A, Voronov A, Gorle PK, Rauscher M, Roosen A, Peukert W. Dispersing and stabilizing silicon nanoparticles in a low-epsilon medium. Colloids Surf A 2008;320(1–3):183–8.
[27] Weast RC, Selby SM, Hodgman CD, editors. CRC Handbook of Chemistry and Physics. 85th ed. Boca Raton, Fl: CRC Press; 2004–05.

[28] Chen Y, Liang Y, Zheng F, Zhou R, Feng Z. The dispersion behavior of Si–C–N nanopowders in organic liquids. Ceram Int 2001;27(1):73–9.
[29] Pei S, Cheng H-M. The reduction of graphene oxide. Carbon 2012;50(9):3210–28.
[30] Chou S-L, Wang J-Z, Choucair M, Liu H-K, Stride JA, Dou S-X. Enhanced reversible lithium storage in a nanosize silicon/graphene composite. Electrochem Commun 2010;12(2):303–6.

Supporting information for

# A Stable Silicon/Graphene Nanocomposite via Solvent Exchange Method as Anode Material in Lithium Ion Battery

*Deniz P. Wong [a,c,d], Han-Ping Tseng [e], Yit-Tsong Chen [b,c], Bing-Joe Hwang [e,*], Li-Chyong Chen[a,*] and Kuei-Hsien Chen [a,b,*]*

[a]Center for Condensed Matter Sciences, National Taiwan University, No. 1 Sec. 4, Roosevelt Rd., Taipei 10617, Taiwan

[b]Institute of Atomic and Molecular Sciences, Academia Sinica, No. 1 Sec. 4, Roosevelt Rd., Taipei 10617, Taiwan

[c]Department of Chemistry, National Taiwan University, No. 1 Sec. 4, Roosevelt Rd., Taipei 10617, Taiwan

[d]Nanoscience and Technology Program, Taiwan International Graduate Program, Academia Sinica, Taipei 11529, Taiwan

[e]Department of Chemical Engineering, National Taiwan University of Science and Technology, 43 Keelung Road, Section 4, Taipei 10617, Taiwan

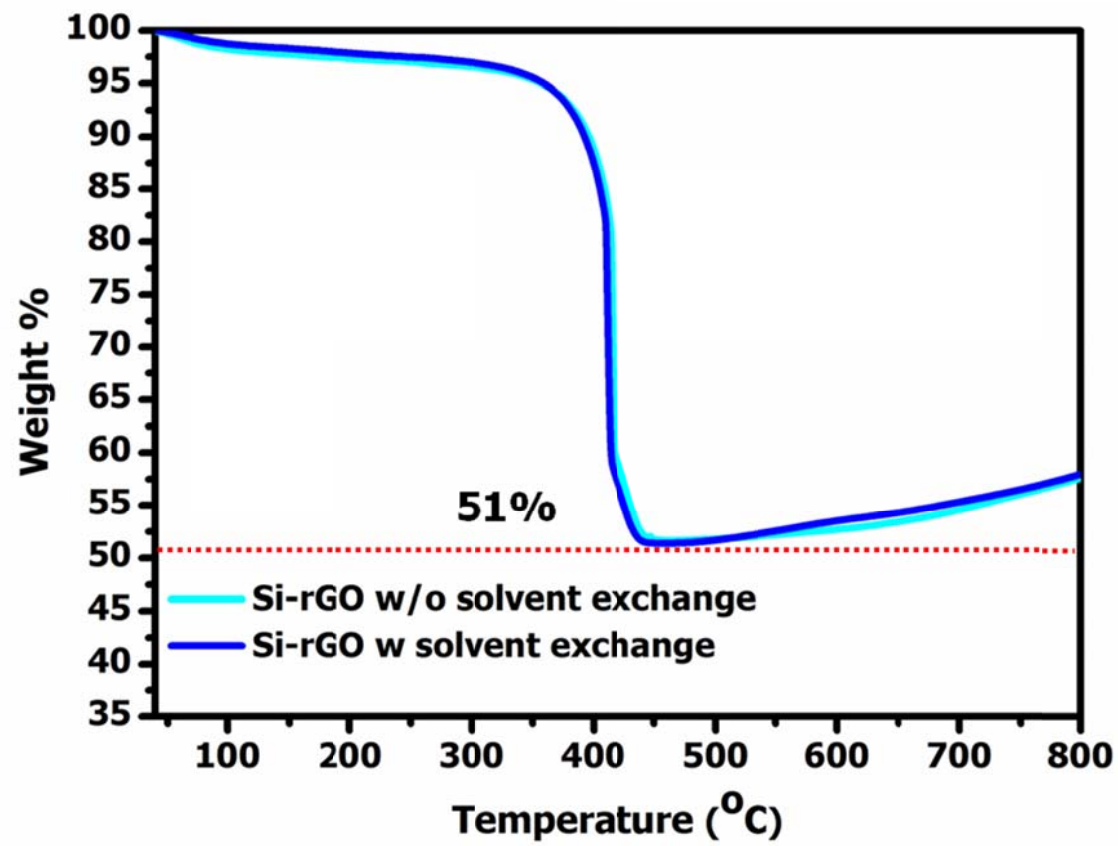


**Fig. S1** - Thermal gravimetric analysis of Si–rGO nanocomposites to determine the amount of silicon present in the material.

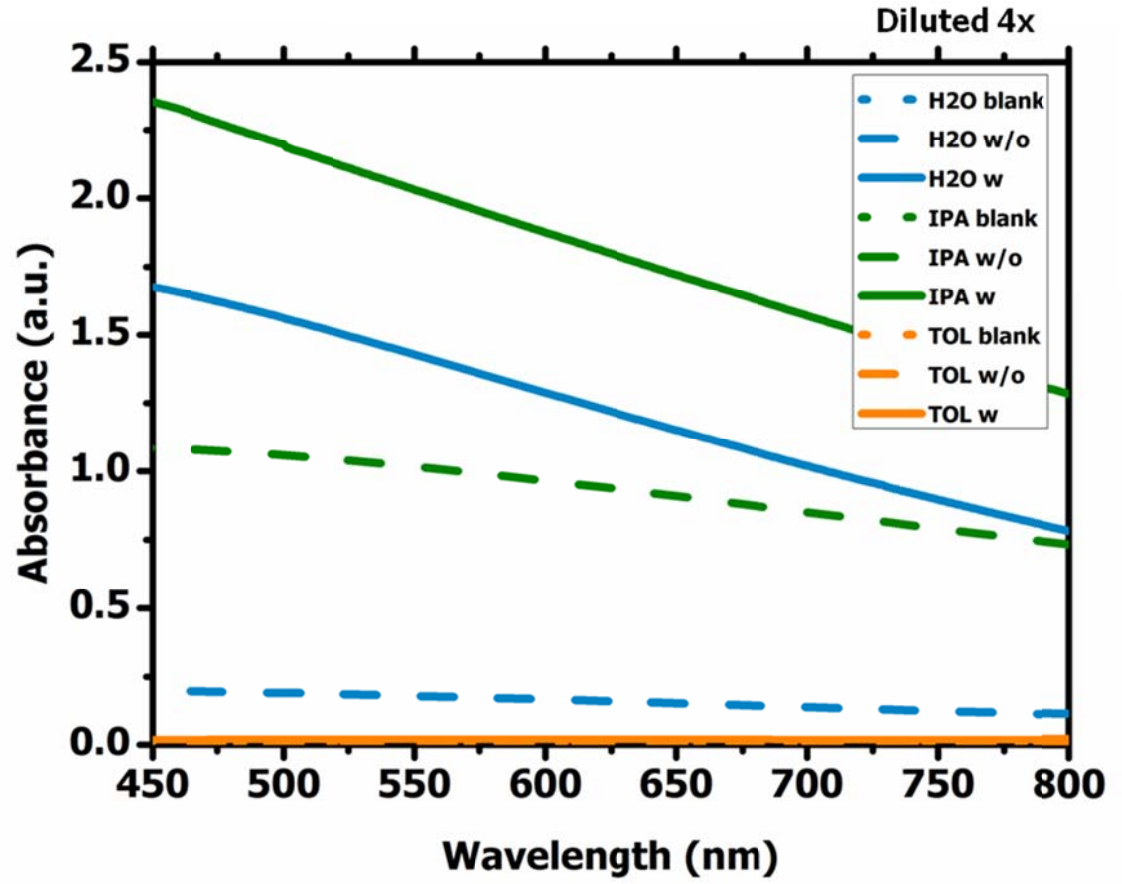


**Fig. S2** - Visible absorption spectra of Si NPs in various solvent after one day. The solutions were diluted 4x. Only 5 spectra can be visibly seen from the figure due to the overlapping of the lines near the zero mark. Aside from the blank runs (H2O blank, IPA blank and TOL blank) which do not contain Si NPs, nearly negligible absorption of Si NPs is observed in toluene as solvent due to sedimentation of Si NPs at the bottom of the cell.

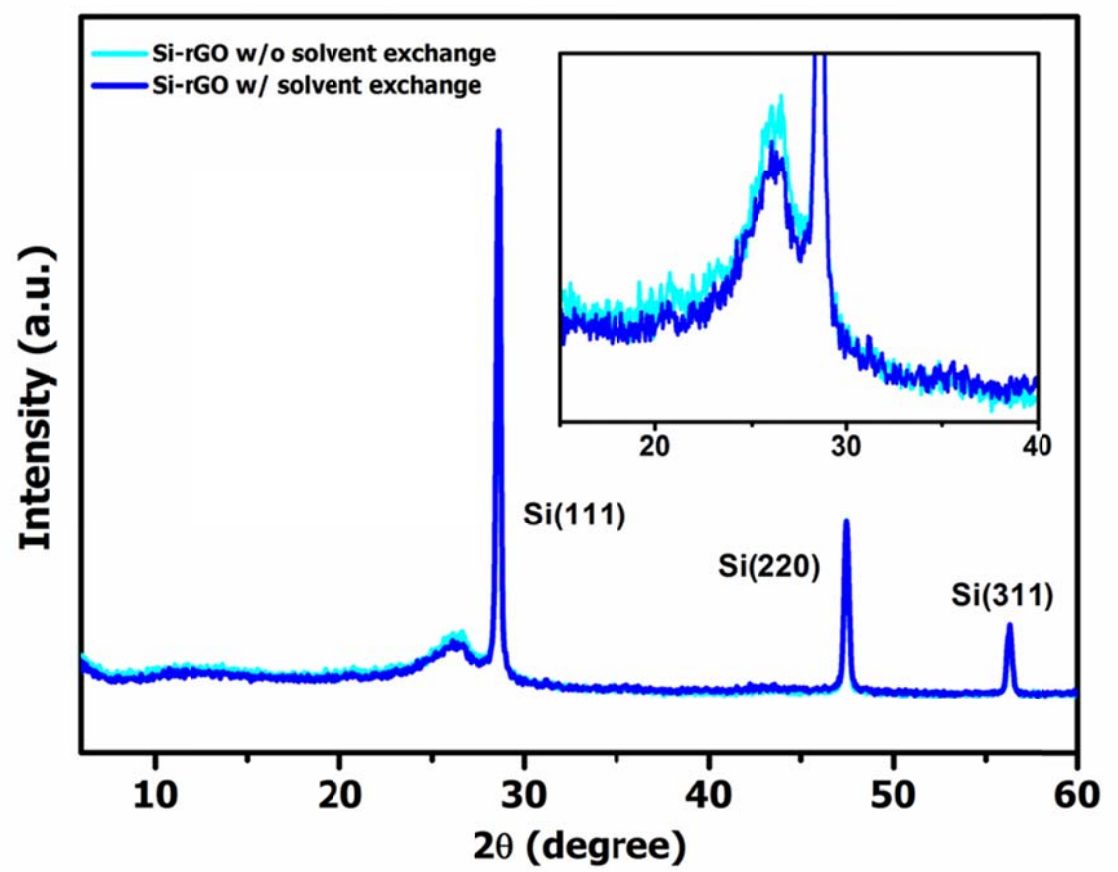


**Fig. S3 -** XRD patterns of Si-rGO nanocomposites with and without Si NPs undergoing the solvent exchange process. Inset: Enlarged portion of the spectra focusing on the graphitic peak after GO reduction.

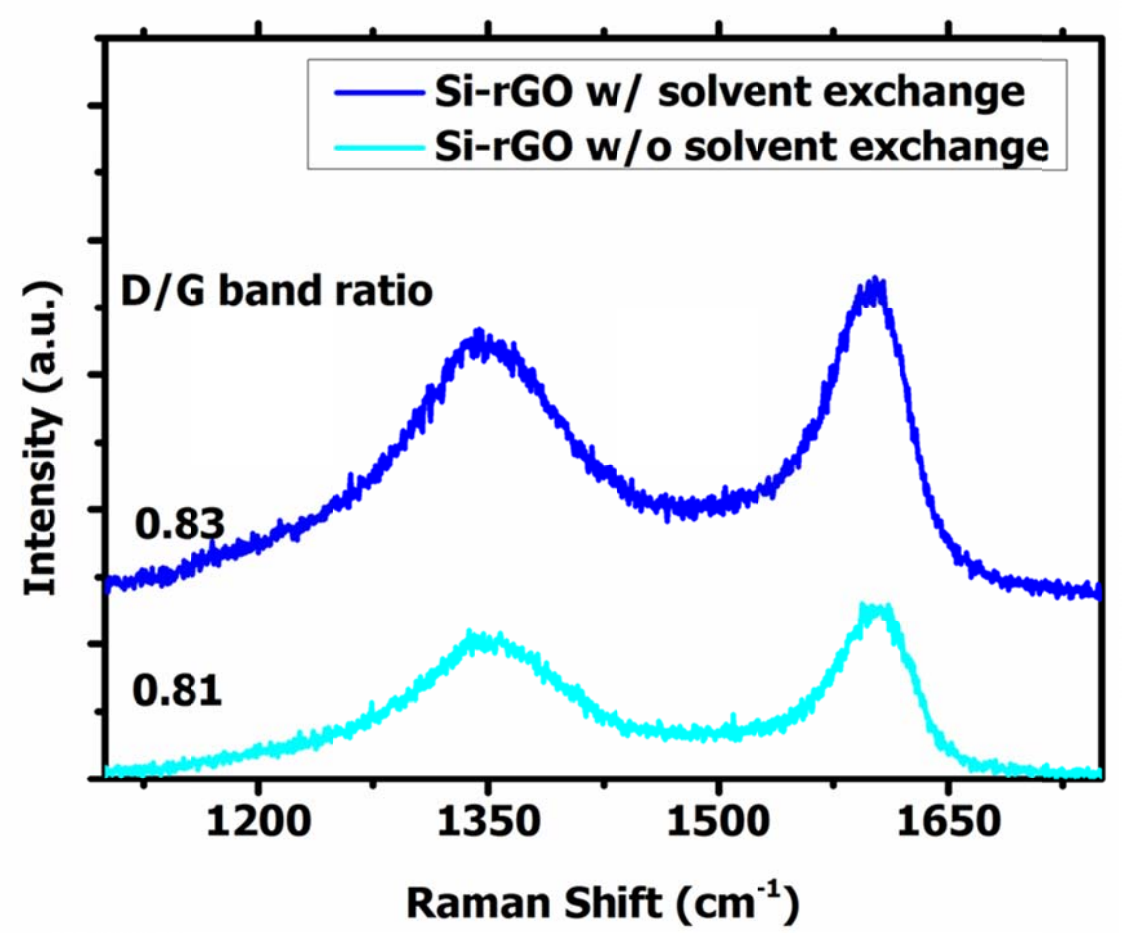


**Fig. S4** - Raman spectra of Si-rGO nanocomposites with and without Si NPs undergoing the solvent exchange process.

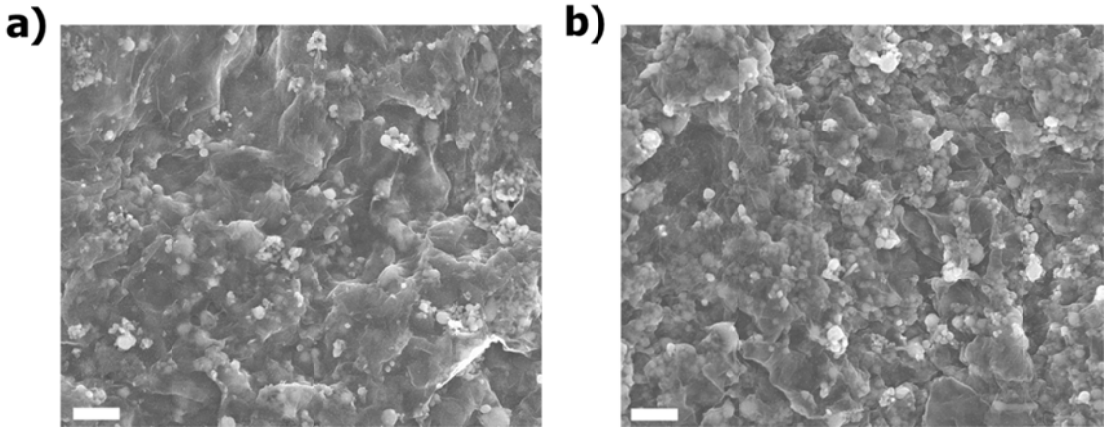


**Fig. S5** - SEM images of Si-rGO nanocomposite a) without and b) with undergoing the solvent exchange process (scale bar: 1 μm)

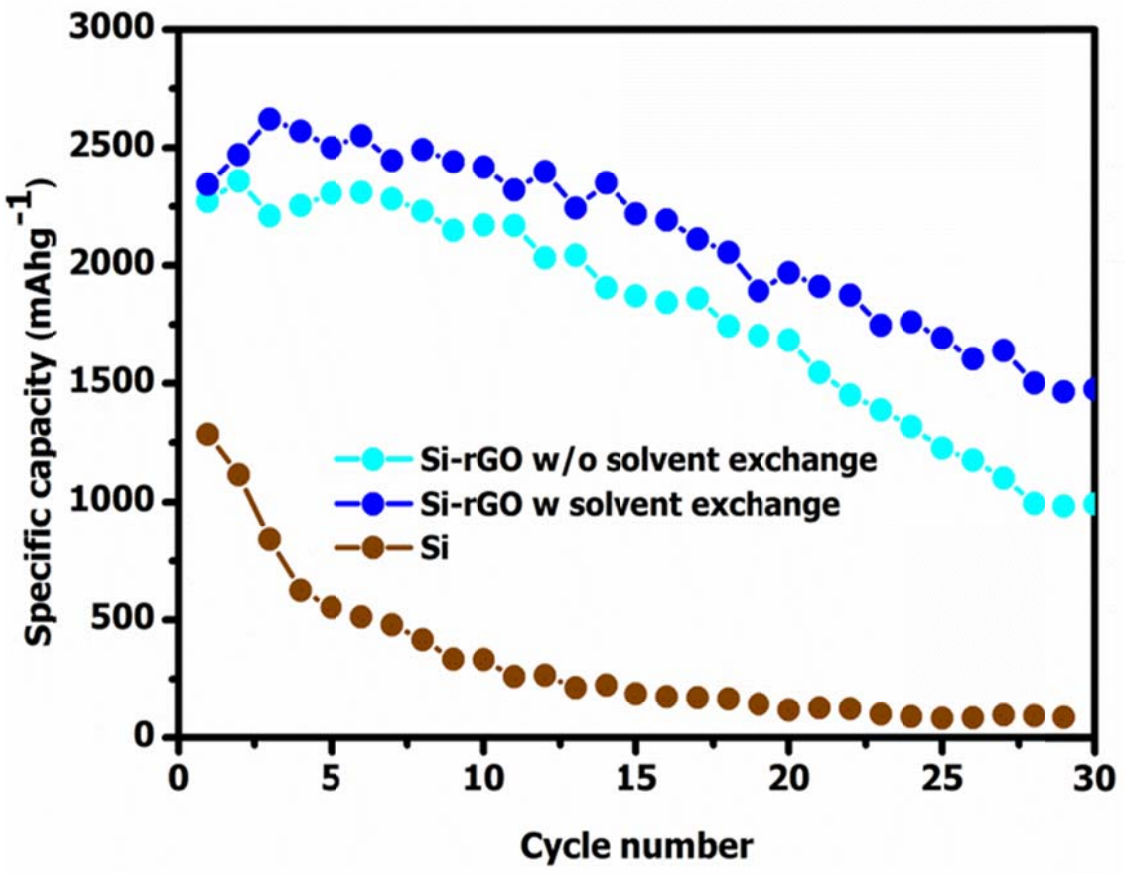


**Fig. S6** - Cycling performance of Si-rGO nanocomposite with and without solvent exchange and pure Si after normalizing the capacity to the weight of silicon.